Integrated feedback ramp metering and mainstream traffic flow control on motorways using variable speed limits

Rodrigo Castelan Carlson[a,*], Ioannis Papamichail[b], Markos Papageorgiou[b]

[a] *Center for Mobility Engineering and Post-graduate Program in Automation and Systems*
Federal University of Santa Catarina
Campus Joinville, 89218-000, Joinville, SC, Brazil
[b] *Dynamic Systems and Simulation Laboratory*
Department of Production Engineering and Management
Technical University of Crete
University Campus, 73100, Chania-Crete, Greece

Abstract

Ramp Metering (RM) is the most direct and efficient tool for the motorway traffic flow management. However, because of the usually short length of the on-ramps, RM is typically deactivated to avoid interference of the created ramp queue with adjacent street traffic. By the integration of local RM with Mainstream Traffic Flow Control (MTFC) enabled via Variable Speed Limits (VSL), control operation upstream of active bottlenecks could be continued even if the on-ramp is full or if the RM lower bound has been reached. Such integration is proposed via the extension of an existing local cascade feedback controller for MTFC-VSL by use of a split-range-like scheme that allows different control periods for RM and MTFC-VSL. The new integrated controller remains simple yet efficient and suitable for field implementation. The controller is evaluated in simulation for a real motorway infrastructure (a ring-road) fed with real (measured) demands and compared to stand-alone RM or MTFC-VSL, both with feedback and optimal control results. The controller's performance is shown to meet the specifications and to approach the optimal control results for the investigated scenario.

Keywords: traffic management, integrated motorway traffic flow control, ramp metering, mainstream traffic flow control, variable speed limits, feedback control, optimal control

1. INTRODUCTION

Traffic flow congestion on motorways is a serious and increasing problem of modern societies. Congestion is known to reduce the nominal capacity of the motorway infrastructure (Papageorgiou and Kotsialos, 2002), with serious impact on travel times, traffic safety, fuel consumption and environmental pollution.

Various traffic management measures have been proposed to alleviate traffic congestion but are known to face limitations. Ramp Metering (RM), for example, is the most direct and efficient tool for motorway traffic flow control but has a major limitation: the created ramp queues should not spill over to the adjacent infrastructure. Because the ramp storage space may be limited, RM is typically released when the ramp queue has covered the whole on-ramp. Thus, RM may delay the onset of congestion, accelerate its dissolution and reduce its space extent, but it may have to be deactivated for most of the peak period due to full ramps (Papamichail et al., 2010).

*Corresponding author
Email address: rodrigo.carlson@ufsc.br (Rodrigo Castelan Carlson)

To overcome these limitations, the integration of different traffic control measures has been investigated in the past, for example RM integrated with route guidance (Kotsialos et al., 2002; Karimi et al., 2004); or RM integrated with variable speed limits (VSL) (Hegyi et al., 2005b,a; Zhang et al., 2006; Chang et al., 2007; Carlson et al., 2010b,a; Lu et al., 2010; Zegeye et al., 2012). Most of these approaches are, however, based on sophisticated methods that may face difficulties in field applications; in some cases even simulation results were not satisfactory. Another approach for integration of RM and VSL called SPECIALIST-RM (Schelling et al., 2011), based on the field-tested VSL strategy SPECIALIST (Hegyi et al., 2008; Hegyi and Hoogendoorn, 2010), deals with the particular case of moving limited-length jams.

Mainstream Traffic Flow Control (MTFC) on motorways by the use of VSL was proposed by Carlson et al. (2010b,a) along with its integration with RM via a sophisticated optimal control approach. These studies have shown that MTFC-VSL can improve motorway performance substantially, particularly when integrated with RM. Because of the limited practicality of the optimal control approach employed, Carlson et al. (2011a) designed, based on the same MTFC concept of Carlson et al. (2010b,a), a simple but efficient feedback controller for MTFC-VSL that is deemed suitable for field implementation, without considering, however, the integration with RM.

In this paper we propose the integration of MTFC-VSL with RM using a feedback control approach. The cascade feedback controller for MTFC-VSL developed by Carlson et al. (2011a) is extended via a split-range-like scheme (Stephanopoulos, 1984) such that MTFC-VSL is only applied when the metered on-ramp storage space is about to be exhausted or if the RM lower bound has been reached. The use of the developed strategy for the case where RM and MTFC-VSL operate with the same control period is relatively straightforward. However, very often the control period for RM is smaller than the control period used for VSL. When distinct control periods are used for RM and MTFC-VSL, additional care should be taken for the integration of these techniques. Therefore, the proposed control strategy also takes into account the possibility of RM and MTFC-VSL operating with distinct control periods. Preliminary results were presented by Carlson et al. (2012a,b, 2013b). Simulation-based investigations for a real motorway network using the second-order macroscopic traffic flow simulator METANET (Messmer and Papageorgiou, 1990) demonstrate the features of the proposed integrated control strategy and compare its efficiency against stand-alone feedback-based RM and feedback-based MTFC-VSL. Simulation results with the optimal control tool AMOC (Kotsialos et al., 2002) are also included.

In the next section, the concepts of motorway traffic management involving RM and MTFC-VSL as well as their integration are briefly reviewed. Section 3 presents a review of the feedback control strategies employed in this paper for RM and MTFC-VSL, and introduces the design of the integrated controller. The feedback controllers are tested and compared in Section 4. Finally, Section 5 concludes the paper.

2. MOTORWAY TRAFFIC MANAGEMENT

This section outlines two motorway traffic management methods, Ramp Metering (RM) (see (Papageorgiou and Kotsialos, 2002) for an overview) and Mainstream Traffic Flow Control (MTFC) (Carlson et al., 2010a), as well as their integration. These techniques are employed to improve traffic conditions on motorways, avoiding the capacity drop at bottlenecks and/or the blocking of off-ramps by the congestion, and the resulting reduction in traffic flow throughput (Papageorgiou and Kotsialos, 2002).

2.1. Ramp Metering

Ramp metering (RM) (see (Papageorgiou and Kotsialos, 2002) for an overview), sketched in Figure 1(a), is useful when the demand d (veh/h) arriving from the on-ramp and the mainstream arriving flow q_{in} (veh/h) upstream of the on-ramp exceed the motorway capacity q_{cap} (veh/h) downstream of the on-ramp, activating the bottleneck. In this case, a capacity drop would occur that could be avoided with RM. Ramp metering consists in metering the inflow of vehicles from the ramp into the motorway by stipulating a ramp flow q_{r} (veh/h) by means of traffic lights (Papageorgiou and Papamichail, 2008), so as to keep the bottleneck outflow q_{out} (veh/h) near the capacity q_{cap}. When the flow at the bottleneck is maximum, the density ρ_{out} (veh/km/lane) at the bottleneck is near the critical density ρ_{cr} (veh/km/lane), to which also corresponds a critical speed v_{cr} (km/h). Since with RM the congestion formation at the bottleneck is avoided, the blocking of off-ramps upstream of the bottleneck by queued vehicles on the motorway is also avoided. On the other hand, RM creates a queue w (veh) at the on-ramp. Since the storage space at the on-ramp is limited by its length, usually some queue management technique is used to avoid the queue exceeding a maximum value $w_{\max}$ (veh) so as to not interfere with traffic of the adjacent road infrastructure.

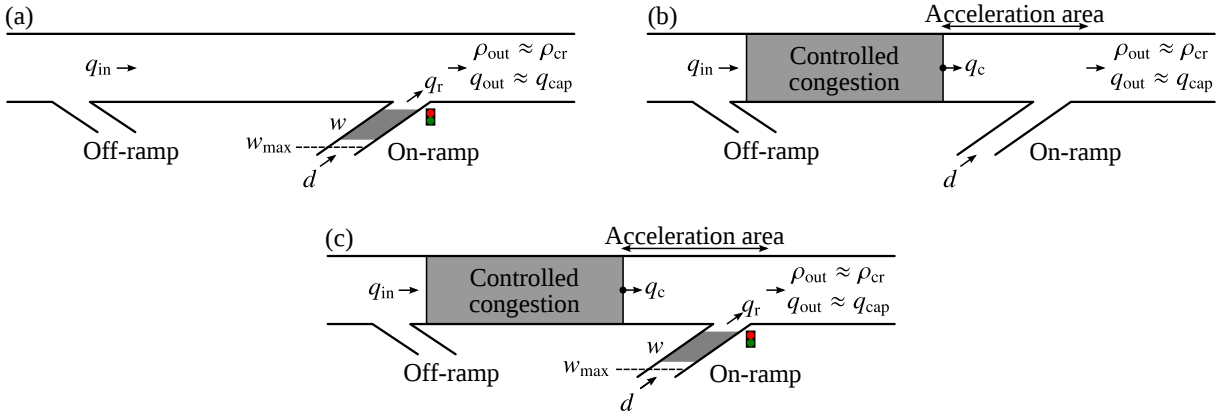

Figure 1: (a) Ramp metering; (b) mainstream traffic flow control; and (c) integrated ramp metering and mainstream traffic flow control.

2.2. Mainstream Traffic Flow Control

The basic idea of Mainstream Traffic Flow Control (MTFC) (Carlson et al., 2010a) is to regulate the arriving mainstream traffic flow q_{in} sufficiently upstream of (otherwise) active bottlenecks (Figure 1(b)). In that way, a controlled congestion is formed on the mainstream with outflow q_{c} (veh/h) and an acceleration area is created between the controlled congestion and the bottleneck area. The acceleration area allows for vehicles that leave the controlled congestion to accelerate and traverse the bottleneck area with critical speed v_{cr}; thus the capacity drop is avoided and maximum bottleneck throughput is achieved. Indeed, the controlled flow q_{c} is defined so that q_{out} equals the bottleneck capacity q_{cap}, whichever is the demand d arriving from the on-ramp (or even in the absence of an on-ramp for other types of bottlenecks). It should be noted that, since the congestion outflow in the MTFC case is higher than in the no-control case, because the capacity drop is avoided, the controlled congestion has a higher internal speed and is space-time shorter than in the no-control case. Hence, less blocking of upstream off-ramps is also expected. In this paper, we use VSL as an MTFC actuator to impose the controlled flow q_{c} on the motorway

mainstream. The area upstream of the acceleration area where VSL is applied is called the VSL application area. For further details, see (Carlson et al., 2010a, 2011a).

2.3. Integrated Motorway Traffic Management

In integrated motorway traffic management, two or more traffic management measures are combined to operate efficiently (Papageorgiou et al., 2003). In the specific case of the integration of RM and MTFC (Figure 1(c)), the idea is to specify a combination of mainstream flow values q_{c} and on-ramp inflows q_{r} so as to keep the bottleneck outflow q_{out} near capacity flow q_{cap}. The advantage from integration is the possibility to keep traffic management operating even if a given restriction of one of the adopted measures has been reached. For example, it is possible to keep MTFC operating even if RM has to be deactivated because of a full ramp. Moreover, the possibility of determining two inflow values, q_{c} and q_{r}, enables the specification of these inflows according to some pre-established criterion, e.g., balancing of waiting time in queues at the ramp and mainstream or balance of queues lengths (Papamichail and Papageorgiou, 2011). Another split policy, which balances the drivers delays on two merging motorways while applying MTFC-VSL to both of them, was proposed by Carlson et al. (2011b).

3. MOTORWAY TRAFFIC FEEDBACK CONTROL

This section outlines two motorway traffic feedback control strategies that are used in the simulations of Section 4, one for RM (including queue management) and another for MTFC-VSL. Then, an integrated feedback control strategy is proposed based on these two strategies.

3.1. PI-ALINEA and queue management

PI-ALINEA (Wang et al., 2014) is a feedback RM strategy corresponding to a Proportional-Integral (PI) controller structure. PI-ALINEA was designed for RM in the case of distant downstream bottlenecks, as an extension of the well known ALINEA strategy (an Integral controller) (Papageorgiou et al., 1991) that is only applicable for bottlenecks just a few hundred meters downstream of the on-ramp nose.

PI-ALINEA orders suitable on-ramp inflows to the motorway based on real-time bottleneck density ρ_{out} measurements as follows:

$$\bar{q}_{\mathrm{r}}(k) = \bar{q}_{\mathrm{r}}(k-1) + \left(\bar{K}_{\mathrm{P}} + \bar{K}_{\mathrm{I}}\right) e_{\rho}(k) - \bar{K}_{\mathrm{P}} e_{\rho}(k-1) \tag{1}$$

with $\bar{q}_{\mathrm{r}}(k)$ (veh/h) the ordered ramp flow to be implemented in the time interval $(kT_{\mathrm{RM}}, (k+1)T_{\mathrm{RM}}]$, T_{RM} (h) the RM control period, and k the discrete-time index; $\bar{q}_{\mathrm{r}}(k)$ is eventually truncated if it exceeds minimum and maximum flow values, i.e., we finally have $\bar{q}_{\mathrm{r}}(k) \in [q_{\mathrm{r,min}}, q_{\mathrm{r,max}}]$; $\bar{K}_{\mathrm{P}}$ and $\bar{K}_{\mathrm{I}}$ are the proportional and integral gains, respectively, and $e_{\rho} = \hat{\rho}_{\mathrm{out}} - \rho_{\mathrm{out}}(k)$ is the density control error with $\hat{\rho}_{\mathrm{out}}$ (veh/km/lane), the set-point, usually set around the critical density ρ_{cr} at which q_{out} is maximised.

The complete feedback control system is depicted in Figure 2(a). The traffic light block corresponds simply to the translation of a desired flow ($\bar{q}_{\mathrm{r}}$) into signal times (e.g., red duration) and then into the flow that leaves the stop line ($\bar{q}'_{\mathrm{r}}$). The possible mismatch between $\bar{q}_{\mathrm{r}}$ and $\bar{q}'_{\mathrm{r}}$ is handled automatically by the feedback structure. The traffic process is modelled by a linearisation of the fundamental diagram around the critical density (see (Papageorgiou

et al., 1991)); it corresponds to the static translation of inflow to the bottleneck into bottleneck density and is given by $K' > 0$. For more details, see (Wang et al., 2014).

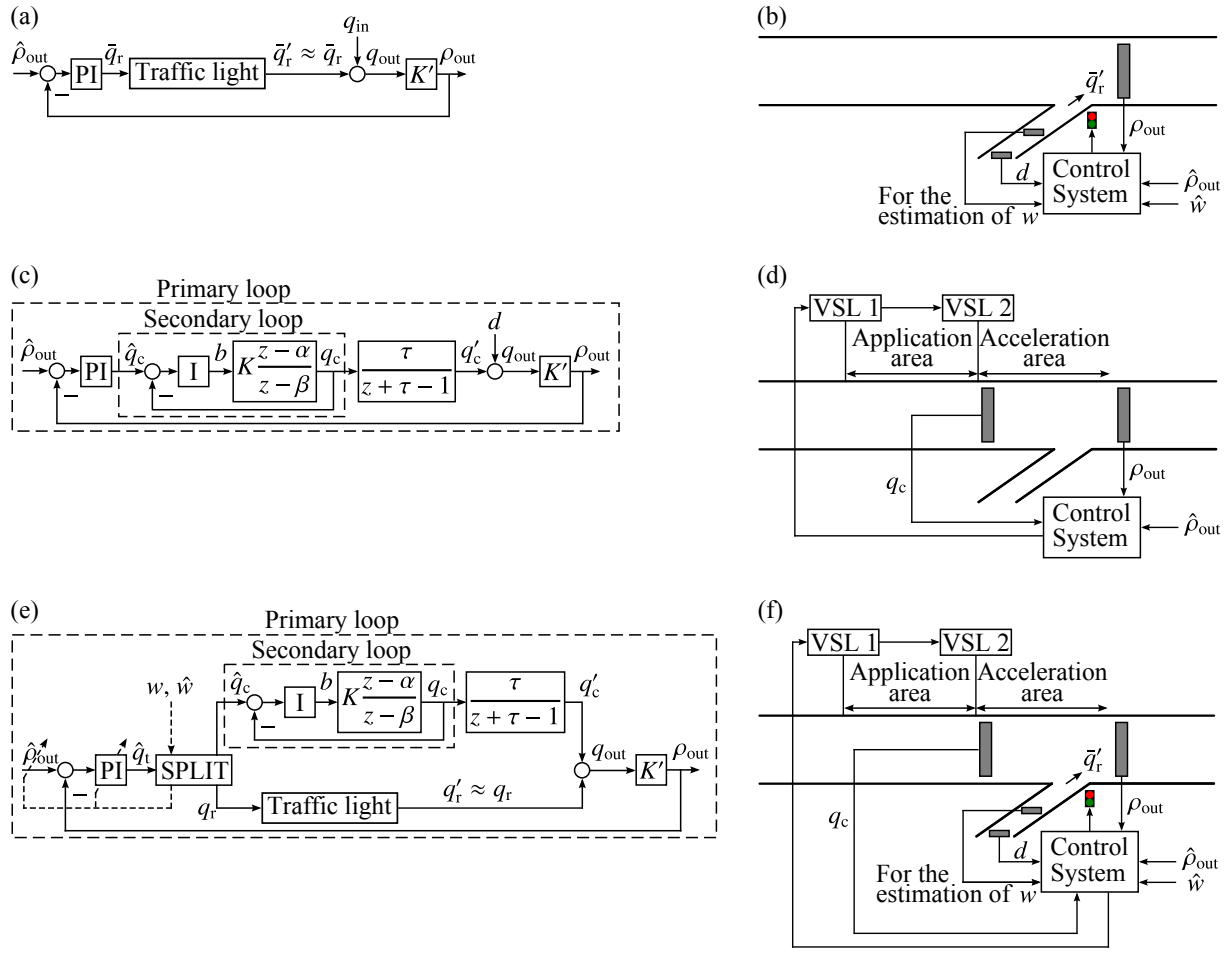

Figure 2: (a) PI-ALINEA (feedback RM); (b) Feedback MTFC-VSL; and (c) feedback integrated control (RM and MTFC-VSL).

When the on-ramp storage space is limited, it is necessary to manage the on-ramp queue in order to keep it within the stipulated limit. Queue management operates in conjunction with RM, overriding the RM ordered inflow to the motorway when necessary to avoid over-long ramp queues. A proportional (P) controller with feed-forwarded on-ramp demand d may be used (Smaragdis and Papageorgiou, 2003):

$$\widehat{q}_{\mathrm{r}}(k) = -\frac{1}{T_{\mathrm{RM}}}\left[\hat{w} - w(k-1)\right] + d(k-1) \tag{2}$$

with $\widehat{q}_{\mathrm{r}}(k)$ (veh/h) the queue-management ordered inflow, which may be truncated to stay bounded within minimum and maximum flow values, i.e., $\widehat{q}_{\mathrm{r}}(k) \in [q_{\mathrm{r,min}}, q_{\mathrm{r,max}}]$; $w(k)$ (veh) is the on-ramp queue length, and $\hat{w} \leq w_{\max}$ is the maximum admissible on-ramp queue (set-point). The final ordered on-ramp inflow to the motorway is $q_{\mathrm{r}} = \max\{\bar{q}_{\mathrm{r}}, \widehat{q}_{\mathrm{r}}\}$. Therefore, we have two controllers; the first, controlling density at the bottleneck, has the purpose of restricting inflow into the motorway to avoid congestion; and the other, controlling ramp queue, works in the opposite direction, releasing flow from the on-ramp to avoid long queues; the higher of both values eventually prevails. Put differently, the flow ordered by queue management serves as a time-varying lower bound for ramp

metering. Note that queue management operates with the same control period as ramp metering, T_{RM}. A PI controller could have been used for queue management as well, see (Sun and Horowitz, 2005a,b).

Figure 2(b) depicts an example of system setup for ramp metering with queue management. The inputs to the control system are the desired density ($\hat{\rho}_{\mathrm{out}}$) and the admissible ramp queue ($\hat{w}$). The bottleneck density (ρ_{out}) is measured for use by PI-ALINEA. The used queue management strategy requires the measurement of the ramp demand (d) and the measurement or estimation of queue length (w). The latter may require a number of sensors, see, e.g., (Vigos et al., 2008). The control system adjusts the traffic signal to determine the inflow ($\bar{q}_{\mathrm{r}}'$) into the motorway.

3.2. Feedback MTFC-VSL

The control problem here is to regulate the traffic density ρ_{out} (Figure 1(b)) via appropriate real-time changes of the mainstream flow q_{c} enabled by VSL (Carlson et al., 2011a). Thus, we have the VSL rate b, which is the ratio of the ordered speed limit divided by the nominal speed limit, as the control action and the bottleneck density ρ_{out} as the controlled variable. Note that in the case depicted in Figure 1(b) the bottleneck is due to a merging on-ramp flow which would represent a disturbance to be rejected by the control loop.

The basis for the design of the feedback MTFC-VSL is a discrete-time linearised model. Figure 2(c) depicts the MTFC feedback cascade controller structure designed by Carlson et al. (2011a). Besides the PI and I controller blocks, to be described next, the diagram depicts three other blocks with α, β, $\tau > 0$, $K' > 0$, and $K > 0$ being model parameters, with $0 < \beta < \alpha \leq 1$; and z the discrete-time complex variable. These blocks describe input-output relations obtained via z-transformation of difference equations (discrete-time counterpart of differential equations) describing dynamic systems (see (Fadali and Visioli, 2013)), in our case the traffic behaviour on the motorway. The first block describes the dynamic behaviour of q_{c} due to a speed limit variation (via VSL rate b), the second block describes the smoothed and delayed propagation of flow through the acceleration area, and the third block is exactly as used before for ALINEA (Section 3.1, Figure 2(a)). A detailed account of the modelling process is provided by Carlson et al. (2011a). The system operation can be summarised as follows: the secondary loop in Figure 2(c) is affected by the VSL rate b delivered by the secondary controller that will determine the outflow q_{c} of Figure 1(b). This flow is measured downstream of the VSL application area and is fed back and compared to the reference flow $\hat{q}_{\mathrm{c}}$ delivered by the primary controller. The primary loop uses the measured density ρ_{out} at the bottleneck area.

The secondary controller of Figure 2(c) was designed as an integral (I) controller:

$$b(k) = b(k-1) + K_{\mathrm{I}} e_q(k) \tag{3}$$

with K_{I} the integral gain and $e_q(k) = \hat{q}_{\mathrm{c}}(k) - q_{\mathrm{c}}(k)$ the flow control error, given per lane and T_{VSL} (h) the MTFC-VSL control period. The primary controller was specified to be a proportional-integral (PI) controller:

$$\hat{q}_{\mathrm{c}}(k) = \hat{q}_{\mathrm{c}}(k-1) + (K_{\mathrm{P}}' + K_{\mathrm{I}}')\, e_\rho(k) - K_{\mathrm{P}}' e_\rho(k-1) \tag{4}$$

with K_{P}' and K_{I}' the proportional and integral gains of the controller, respectively. Similarly to RM, the density set-point $\hat{\rho}_{\mathrm{out}}$ may be set equal to the critical density ρ_{cr} for maximum throughput. For more details about the controller design, tuning and operation, the reader is referred to (Carlson et al., 2011a).

The MTFC-VSL control system (Figure 2(d) requires as input the desired density ($\hat{\rho}_{\text{out}}$) and the measurements of bottleneck density (ρ_{out}) and outflow (q_{c}) of the application area. A VSL sign posts the decisions of the control system (corresponding to VSL rate b) at the entrance of the application area and is identified in the figure by VSL 1. A second speed limit should be posted at the entrance of the acceleration area informing drivers that they are allowed to accelerate to higher speed. This speed limit, identified in the figure by VSL 2, could be a fixed speed limit or, as used in this work, a second VSL with posted speed limit according to rules described by Carlson et al. (2011a). It should be noted that in the simulations of Section 4, VSL is applied to a whole link because of the characteristics of the macroscopic model used. This last aspect is further discussed by Müller et al. (2013).

3.3. Integrated Motorway Traffic Control

The integrated control structure is presented next followed by considerations on how to handle distinct values of control periods for RM and MTFC-VSL.

3.3.1. Control structure

Similarly to the two previously presented approaches for RM and MTFC-VSL, the idea in the integrated case is to specify combined mainstream flow and on-ramp flow values in order to keep the bottleneck density ρ_{out} around the critical density (set-point), so that the outflow q_{out} is maximised (Figure 1(c)). Since there are now two input flows (q_{c} and q_{r}) to control the bottleneck density, there is an additional degree of freedom that may be used to apply some desired policy. The policy pursued in this paper is to apply RM for as long as possible the ramp storage space is not full; and to switch to MTFC-VSL only when ramp queue management is activated, i.e., ramp storage space is about to be exhausted, or when RM lower bound has been reached. This policy may be implemented if the feedback cascade control structure of Figure 2(c) is extended via an appropriate split-range-like control scheme (Stephanopoulos, 1984), as depicted in Figure 2(e). Figure 2(f) indicates that, in terms of system setup, the integrated control system is a combination of the two previous systems.

In Figure 2(e) the PI controller of the primary loop delivers a reference flow $\hat{q}_{\text{t}}$ (veh/h), i.e., the total desired inflow into the bottleneck:

$$\hat{q}_{\text{t}}(k) = \hat{q}_{\text{t}}(k-1) + \left(\hat{K}_{\text{P}} + \hat{K}_{\text{I}}\right) e_{\rho}(k) - \hat{K}_{\text{P}} e_{\rho}(k-1) \tag{5}$$

that is bounded by the sum of the mainstream capacity ($q^{\text{m}}_{\text{cap}}$ (veh/h)) and of the on-ramp capacity ($q^{\text{r}}_{\text{cap}}$ (veh/h)), with $\hat{K}_{\text{P}}$ and $\hat{K}_{\text{I}}$ the proportional and integral gains of the controller, respectively, and T_{c} (h) the control period of the integrated controller. The total desired inflow $\hat{q}_{\text{t}}$ is split into the desired mainstream flow $\hat{q}_{\text{c}}$, which is handled by the MTFC-VSL secondary loop (as in Figure 2(e)), and the desired on-ramp flow q_{r} which is directly implemented via an appropriate metering policy (Papageorgiou and Papamichail, 2008) of the traffic lights to produce the real respective outflows q'_{c} and q'_{r} that enter the bottleneck area.

The operation of the split block is relatively simple. Any change of $\hat{q}_{\text{t}}$ ordered by the primary controller is conveyed to q_{r}, unless one of two restrictions apply: i) the lower RM bound $q_{\text{r,min}}$ has been reached, or ii) the queue management orders a higher value, in which case the final RM ordered flow q_{r} is set equal to $\widehat{q}_{\text{r}}$. In either of the two cases, any ordered flow changes are transmitted to $\hat{q}_{\text{c}}$. Recall from Section 3.1 that the queue management ordered

case $\hat{q}_{\mathrm{t}} \geq q^{\mathrm{m}}_{\mathrm{cap}} + \widehat{q}_{\mathrm{r}}$ // No restriction
    $q_{\mathrm{r}} = \hat{q}_{\mathrm{t}} - q^{\mathrm{m}}_{\mathrm{cap}}$
    $\hat{q}_{\mathrm{c}} = q^{\mathrm{m}}_{\mathrm{cap}}$
otherwise // Full ramp or ramp ordered flow reached lower bound
    $q_{\mathrm{r}} = \widehat{q}_{\mathrm{r}}$
    $\hat{q}_{\mathrm{c}} = \hat{q}_{\mathrm{t}} - \widehat{q}_{\mathrm{r}}$
end

Algorithm 1: Split of $\hat{q}_{\mathrm{t}}$ between q_{r} and $\hat{q}_{\mathrm{c}}$.

flow absorbs the lower RM bound resulting in a single restriction. More precisely, we have $\hat{q}_{\mathrm{t}} \leq q^{\mathrm{m}}_{\mathrm{cap}} + q^{\mathrm{r}}_{\mathrm{cap}}$, and the split of $\hat{q}_{\mathrm{t}}$ between q_{r} and $\hat{q}_{\mathrm{c}}$ is given by Algorithm 1.

In essence, the controller operates as PI-ALINEA until the restriction applies, at which point it starts operating as MTFC-VSL, and $\widehat{q}_{\mathrm{r}}$ becomes a feed-forward element affecting the output of the primary controller.

To further clarify the method, Figure 3 sketches the time series of the variables used in the splitting operation of the integrated controller for two hypothetical scenarios. First, consider the scenario of Figure 3(a) in which queue management is disabled and $q_{\mathrm{r,min}} = 0$, i.e., the restriction corresponds to the constant lower RM bound, and MTFC-VSL will be activated only after full closure of the on-ramp. The desired inflow $\hat{q}_{\mathrm{t}}$ is allowed to vary from $q^{\mathrm{m}}_{\mathrm{cap}} + q^{\mathrm{r}}_{\mathrm{cap}}$ (top dashed gray line) to zero. Note that this range for $\hat{q}_{\mathrm{t}}$ corresponds to the sum of capabilities of each actuator and not of the infrastructure (which is, at the bottleneck, $q^{\mathrm{m}}_{\mathrm{cap}}$). The split of $\hat{q}_{\mathrm{t}}$ must respect the individual limits of each actuator, i.e., $0 = q_{\mathrm{r,min}} \leq q_{\mathrm{r}} \leq q^{\mathrm{r}}_{\mathrm{cap}}$ for RM and $0 \leq \hat{q}_{\mathrm{c}} \leq q^{\mathrm{m}}_{\mathrm{cap}}$ for MTFC-VSL. These two ranges are marked on the right side of the figure by the labelled brackets as if they were stacked (separated by the bottom dashed gray line at $q^{\mathrm{m}}_{\mathrm{cap}}$) with the RM range shifted up by $q^{\mathrm{m}}_{\mathrm{cap}}$. The solid gray curve in the figure corresponds to $\hat{q}_{\mathrm{t}}$ and is at its maximum from time 0 to t_1. As a consequence, the values of q_{r} (black dashed curve shifted by $q^{\mathrm{m}}_{\mathrm{cap}}$) and $\hat{q}_{\mathrm{r}}$ (dotted black curve) are also at their respective maxima. At t_1 the value of $\hat{q}_{\mathrm{t}}$ starts decreasing and, following our policy, we should convey these changes to q_{r}, unless the restriction mentioned above applies. Immediately before t_1, we have $q_{\mathrm{r}} = q^{\mathrm{r}}_{\mathrm{cap}}$, which is clearly above zero (the lower bound), i.e, the restriction does not apply. Hence, we see that the shifted q_{r} curve coincides exactly with the $\hat{q}_{\mathrm{t}}$ curve until time t_2, and one can verify from the figure that $q_{\mathrm{r}} = \hat{q}_{\mathrm{t}} - q^{\mathrm{m}}_{\mathrm{cap}}$. Meanwhile, from t_1 to t_2, MTFC-VSL is clearly not needed and $\hat{q}_{\mathrm{c}}$ remains unchanged with value $q^{\mathrm{m}}_{\mathrm{cap}}$. At time t_2, the amount of flow reduction in $\hat{q}_{\mathrm{t}}$ equals $q^{\mathrm{r}}_{\mathrm{cap}}$ and, since $\hat{q}_{\mathrm{t}}$ changes were conveyed to q_{r}, its value is zero and the lower bound has been reached. The restriction applies and, according to the policy, further changes to $\hat{q}_{\mathrm{t}}$ should be conveyed to $\hat{q}_{\mathrm{c}}$ until the restriction does not apply anymore.

From time t_2 onward, $\hat{q}_{\mathrm{c}}$ is seen to be changing by the same amount as $\hat{q}_{\mathrm{t}}$ and, as a matter of fact, their values are identical, $\hat{q}_{\mathrm{c}} = \hat{q}_{\mathrm{t}}$. Indeed, if no flow is entering from the on-ramp, and $\hat{q}_{\mathrm{t}}$ is the total desired inflow, this flow should enter from the mainstream. This condition is true until t_3 when MTFC-VSL is not needed anymore. The values found for $\hat{q}_{\mathrm{c}}$ and q_{r} from 0 to t_1 and from t_1 to t_2 are exactly the values given by the algorithm if $\widehat{q}_{\mathrm{r}} = 0$. Recall from Section 3.1 that queue management works as a time-varying lower bound for ramp metering. This means that, when queue management is disabled, the lower bound is constant and equal to $q_{\mathrm{r,min}}$ (in this example equal to zero) and therefore $\widehat{q}_{\mathrm{r}} = 0$. A straight consequence is that the condition in Algorithm 1 becomes $\hat{q}_{\mathrm{t}} \geq q^{\mathrm{m}}_{\mathrm{cap}} + q_{\mathrm{r,min}} = q^{\mathrm{m}}_{\mathrm{cap}}$

and allows an easy interpretation of its role in the method. The difference $\hat{q}_\mathrm{t} - q^\mathrm{m}_\mathrm{cap}$ is simply the amount of flow that could be reduced by RM before reaching the lower bound. Therefore, if $\hat{q}_\mathrm{t}$ is greater than the shifted lower bound $(0 + q^\mathrm{m}_\mathrm{cap})$, q_r can still be reduced, otherwise MTFC-VSL is needed as we see at t_2 exactly when the $\hat{q}_\mathrm{t}$ curve crosses with the shifted q_r lower bound.

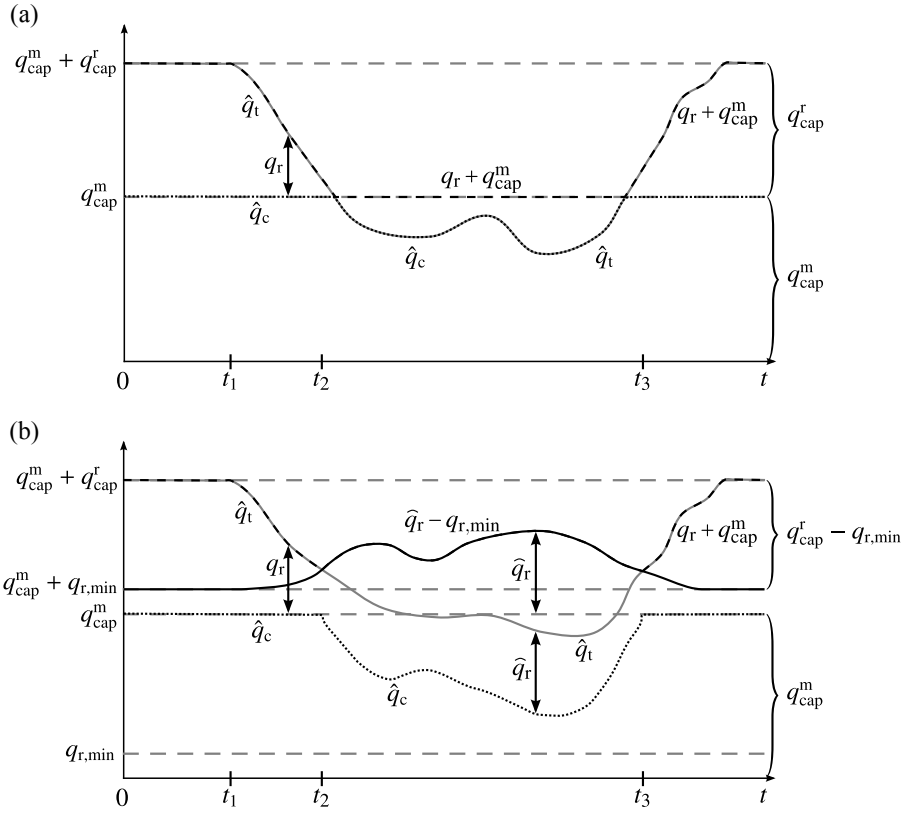

Figure 3: Time series of the variables used in the splitting operation of the integrated controller for two hypothetical scenarios: (a) queue management is disabled and $q_\mathrm{r,min} = 0$; and (b) queue management is enabled and $q_\mathrm{r,min} \neq 0$.

A scenario with enabled queue management and $q_\mathrm{r,min} \neq 0$ is sketched in Figure 3(b). The structure of the figure is pretty similar to Figure 3(a), but the range of values for $\hat{q}_\mathrm{t}$ is bottom-limited by $q_\mathrm{r,min}$ (bottom-dashed gray curve). A dashed gray line also indicates $q_\mathrm{r,min}$ shifted up by $q^\mathrm{m}_\mathrm{cap}$ reducing the possible values of q_r. Another addition to the figure is curve of $\widehat{q}_\mathrm{r}$ shifted up by $q^\mathrm{m}_\mathrm{cap}$ (black solid). This curve has the role of a shifted time-varying lower bound. Following the same reasoning applied to the previous figure, from 0 to t_1 the ordered flows $\hat{q}_\mathrm{t}$, q_r, and $\hat{q}_\mathrm{c}$ are all at their respective maximum values, i.e., no control is needed. From t_1 onward, $\hat{q}_\mathrm{t}$ decreases, and the same amount of change is conveyed to q_r. At t_2 the $\hat{q}_\mathrm{t}$ curve crosses the shifted $\widehat{q}_\mathrm{r}$ curve indicating that the queue management restriction applies. The restriction remains from t_2 to t_3, and, during this period, any changes in $\hat{q}_\mathrm{t}$ are conveyed to $\hat{q}_\mathrm{c}$. Note however that, meanwhile, $\widehat{q}_\mathrm{r}$ is also changing, and these changes should also be conveyed to $\hat{q}_\mathrm{c}$. In summary, from 0 to t_2 we have $\hat{q}_\mathrm{t} - q^\mathrm{m}_\mathrm{cap} \geq \widehat{q}_\mathrm{r}$, whereas from t_2 to t_3 the opposite is true, and one can verify from the figure that for each condition the values of q_r and $\hat{q}_\mathrm{c}$ match those of Algorithm 1.

The proposed algorithm may be modified to use the measurements of q_c and q'_r to speed up the controller reaction in a way similar to what is proposed for ramp metering by Wang et al. (2014). This can be handled with

additional coding but does not affect the essence of the method.

Clearly, the operating gains of the primary controller should be scheduled based on the split decision, i.e., $\bar{K}_\mathrm{P}$ and $\bar{K}_\mathrm{I}$ (PI-ALINEA gains) are used if the first condition in Algorithm 1 applies, otherwise K'_P and K'_I (MTFC-VSL gains) are used. Similarly, the set-point $\hat{\rho}_\mathrm{out}$ of the primary controller must be changed accordingly, if VSL is applied at the bottleneck area in the MTFC case, since lower VSL values shift the critical density to higher values (Papageorgiou et al., 2008; Carlson et al., 2010b).

Note that the use of a PI controller during the prevalence of the first condition is not an imposition. Actually, the integral gain could be set appropriately and the proportional gain set to zero, in which case the primary controller would operate as ALINEA.

3.3.2. Handling different control periods

The operation of the integrated controller based on (5) and Algorithm 1 may be applied directly if the control periods used for RM, T_RM, and for MTFC-VSL, T_VSL, are identical, i.e., $T_\mathrm{c} = T_\mathrm{RM} = T_\mathrm{VSL}$, as used by Carlson et al. (2012a,b). However, the suggested value by Carlson et al. (2011a, 2013a) for T_VSL is 60 s, while Papageorgiou and Papamichail (2008) suggest $T_\mathrm{RM} \leq 60$ s, being preferred the adoption of smaller values for T_RM.

When $T_\mathrm{RM} \neq T_\mathrm{VSL}$, the value of T_c must be switched to T_RM or T_VSL according to the conditions in Algorithm 1. Due to the switch in the value of the control period, additional care should be taken since the frequency of application of (5) is affected accordingly. The treatment for the problem of switching the control period adopted in this paper is based on the approach described by Fadali and Visioli (2013) and originally proposed by Albertos et al. (2003). In some control systems with variable control period, the lengths of the control period are defined and updated in real-time with the purpose of saving scarce computational resources. As the set of possible control periods may not be known, the control gains, which are dependent on the control period, cannot be defined in advance. Likewise, past values of the involved variables that may be needed by the control law cannot be stored since this would require an infinite storage space. For our specific problem these two aspects can be summarized as follows:

1. the values of $\hat{K}_\mathrm{P}$ and $\hat{K}_\mathrm{I}$ in (5) depend on the control period T_c being used (see (Fadali and Visioli, 2013)); and
2. equation (5) requires past values of the density error e_ρ and of the control action $\hat{q}_\mathrm{t}$ that may not be available for the new control period, since these values may not have been stored or calculated for past time instants spaced according to the control period currently in use.

In the following we develop the solution for these problems for the case when $T_\mathrm{VSL} = 2T_\mathrm{RM}$, with the advantage that the values of the control periods are typically pre-determined and the computational resources are not too limited. A similar approach can be followed for other multiples of T_RM (Albertos et al., 2003).

With respect to Aspect 1 above, the gains of the controller may be defined as a function of the control period T_c and be recalculated every time the control period is switched. For the integrated control case, the dynamics of the controlled system changes (see Figure 2(e)) and the values of gain and control periods for RM and MTFC-VSL are predefined. Thus, it suffices to change directly the values of gains as proposed in Section 3.3.1, without the need for online calculations.

With respect to Aspect 2, two cases are considered separately. First, the case in which the control period is reduced, i.e., T_{c} is switched from T_{VSL} to T_{RM}; and then the case in which the control period is increased, i.e., T_{c} is switched from T_{RM} to T_{VSL}.

Figure 4(a) depicts the case in which the control period is reduced. In the time axis t the time instants for MTFC-VSL and the equivalent time instants in case RM was under operation are shown. In the figure, the curves of the density control error e_ρ and total ordered flow $\hat{q}_{\mathrm{t}}$ are shown, the latter with variations at every T_{VSL}. Indeed, the time instants for MTFC-VSL are spaced by T_{VSL} and only at these time instants the control algorithm stores the value of e_ρ and calculates the value of $\hat{q}_{\mathrm{t}}$. The switch of the control period occurs at time kT_{VSL} (kT_{RM}). If there was no switch of the control period at time instant kT_{VSL}, the values $e_\rho(kT_{\mathrm{VSL}})$, $e_\rho((k-1)T_{\mathrm{VSL}})$, and $\hat{q}_{\mathrm{t}}((k-1)T_{\mathrm{VSL}})$ would be used for the calculation of $\hat{q}_{\mathrm{t}}(kT_{\mathrm{VSL}})$, according to (5). Instead, since the control period is switched at this time instant, the values $e_\rho(kT_{\mathrm{RM}})$, $e_\rho((k-1)T_{\mathrm{RM}})$, and $\hat{q}_{\mathrm{t}}((k-1)T_{\mathrm{RM}})$ are needed for the calculation of $\hat{q}_{\mathrm{t}}(kT_{\mathrm{RM}})$. Note, however, that the time instant $(k-1)$ for MTFC-VSL does not coincide with the time instant $(k-1)$ for RM, because the control periods are different, whereas the time index k at kT_{RM} and kT_{VSL} is the same by definition (see Figure 4(a)).

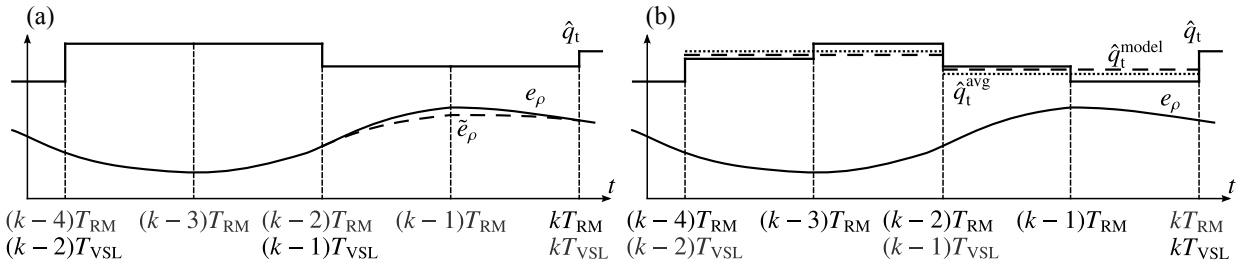

Figure 4: Control period switch with $T_{\mathrm{VSL}} = 2T_{\mathrm{RM}}$: (a) from T_{VSL} to T_{RM}; and (b) from T_{RM} to T_{VSL}.

When looking at Figure 4(a), and since we need the value of $\hat{q}_{\mathrm{t}}(kT_{\mathrm{RM}})$, the values corresponding to the time line of RM should be used. Because $\hat{q}_{\mathrm{t}}$ remains constant during the interval $[(k-2)T_{\mathrm{RM}}, kT_{\mathrm{RM}})$ ($[(k-1)T_{\mathrm{VSL}}, kT_{\mathrm{VSL}})$), the value of $\hat{q}_{\mathrm{t}}((k-1)T_{\mathrm{RM}})$ is known, since it is equal to $\hat{q}_{\mathrm{t}}((k-1)T_{\mathrm{VSL}})$, and can be used directly. The value of $e_\rho((k-1)T_{\mathrm{RM}})$, on the other hand, is not known and could be estimated, for example, by interpolation (Fadali and Visioli, 2013), as sketched in Figure 4(a) by the dashed line, in which $\tilde{e}_\rho$ is the estimated error. Since in this type of application computation resources is not a main concern, we opted to store e_ρ at every T_{RM} even when MTFC-VSL is under operation. Thus, in the moment of the switch $e_\rho((k-1)T_{\mathrm{RM}})$ can be used directly.

Figure 4(b) depicts the analogous case in which the control period is increased. In the time axis t, the time instants for RM and the equivalent time instants in case MTFC-VSL was under operation are shown. In the figure, the curves of the density control error e_ρ and total ordered flow $\hat{q}_{\mathrm{t}}$ are shown, the latter with variations at every T_{RM}. In contrast to the previous case, the time instants for RM, spaced by T_{RM}, occur more often than MTFC-VSL time instants. Since at every T_{RM} the control algorithm stores the value of e_ρ and calculates the value of $\hat{q}_{\mathrm{t}}$, apparently all needed values could be available when switching from T_{RM} to T_{VSL}. Unfortunately, the switching is still not as straightforward as that because the past control action with MTFC-VSL that would lead to the current state is likely not to be the same past control action from T_{RM}, as discussed next. The switch of the control period occurs at

time kT_{RM} (kT_{VSL}). The values from the time line of MTFC-VSL should be used for the calculation of $\hat{q}_{\mathrm{t}}(kT_{\mathrm{VSL}})$. In this case, the value of $\hat{q}_t$ is not constant during the interval $[(k-1)T_{\mathrm{VSL}}, kT_{\mathrm{VSL}})$. Hence, one would have to find out which value of $\hat{q}_t$ constant over the whole period, and based on the values available at $(k-1)T_{\mathrm{VSL}}$, would lead the system to the actual state. This value can be calculated, approximately, using a mathematical model of the system as the one in Figure 2(e) (Fadali and Visioli, 2013) and is illustrated by the dashed line in Figure 4(b), in which $\hat{q}_{\mathrm{t}}^{\mathrm{model}}$ is the value obtained from the model and the measurements at $(k-1)T_{\mathrm{VSL}}$. However, this would require the knowledge of the model parameters α, β, τ, K' and K that in this specific application may be difficult to determine (Carlson et al., 2011a). Instead, for this work, we opted to follow the approach by Pohjola (2009) that uses the average of the values of $\hat{q}_{\mathrm{t}}$ in the interval $[(k-2)T_{\mathrm{RM}}, kT_{\mathrm{RM}})$, yielding a value $\hat{q}_{\mathrm{t}}^{\mathrm{avg}}$ for the whole interval, indicated by the dotted line in the figure. Finally, since the measurements of e_ρ coincide for RM and MTFC-VSL at every $2T_{\mathrm{RM}}$, $e_\rho((k-1)T_{\mathrm{VSL}}) = e_\rho((k-2)T_{\mathrm{RM}})$ can be used in (5) (Figure 4(b)).

4. SIMULATION RESULTS

A number of different control scenarios are examined in the following, using the METANET simulator (Messmer and Papageorgiou, 1990) for no-control and feedback control cases, and AMOC (Kotsialos et al., 2002) for optimal control. The simulated scenarios and respective results are summarized in Table 1.

Because stand-alone RM or MTFC-VSL using either of the two control approaches, i.e., feedback or optimal control, have been thoroughly investigated in previous works for the same motorway network (Papamichail et al., 2010; Carlson et al., 2010a, 2013c), the related detailed results of optimal control (AMOC) are omitted, except for the integrated case and for the resulting TTS for all scenarios with optimal control that are provided in the table as a reference of achievable performance.

4.1. Amsterdam Ring-road

For this study, the counter-clockwise direction of the Amsterdam ring-road (A10), as depicted in Figure 5, is considered. This motorway is about 32 km long, with 21 on-ramps and 20 off-ramps, including the motorway-to-motorway junctions with A1, A2, A4 and A8. The merge area of A1 with A10 in link L107 (on-ramp OA1) is the main recurrent bottleneck of this motorway for the afternoon peak period considered here. The model parameters were determined via validation with real data (Kotsialos et al., 2002), while VSL-specific model parameters were chosen so that a capacity increase is not induced (Carlson et al., 2010a).

The study was realized for a time horizon of 4 h and the used demand reflects the afternoon peak. The minimum admissible VSL rate is $b_{\min} = 0.2$ and the minimum admissible RM rate is $q_{\mathrm{r,min}} = 200$ veh/h. The control periods, that determine the frequency of posted VSL changes and RM rate updates, are chosen as $T_{\mathrm{VSL}} = 60$ s for MTFC-VSL and $T_{\mathrm{RM}} = 30$ s for RM (see Section 3.3.2), except otherwise stated. The simulation model time step is $T = 10$ s.

4.2. No Control

For the case in which the ring-road is simulated without control measures, the density and the flow at the bottleneck (L107) and the queue at the on-ramp OA1 are shown in Figure 6(a). The excessive demand causes

Table 1: Summary of simulated scenarios.

Scenario	Description	TTS (veh·h)	%
No-control	-	14,163	-
RM-AMOC	Optimal ramp metering without restriction on the queue length at the on-ramp; T_{RM} = 30 s.	7,266	−48.7
RM-FB	Feedback ramp metering without restriction on the queue length at the on-ramp; T_{RM} = 30 s.	7,339	−48.2
RM/Q-AMOC	Optimal ramp metering with restriction on the queue length at the on-ramp (200 veh); T_{RM} = 30 s.	12,062	−14.8
RM/Q-FB	Feedback ramp metering with restriction on the queue length at the on-ramp (200 veh); T_{RM} = 30 s.	12,667	−10.6
MTFC-AMOC	Optimal mainstream traffic flow control via variable speed limits; T_{VSL} = 60 s.	8,009	−43.4
MTFC-FB	Feedback mainstream traffic flow control via variable speed limits; T_{VSL} = 60 s.	9,513	−32.8
IC-AMOC	Optimal integrated control; T_{RM} = 30 s and T_{VSL} = 60 s.	7,184	−49.3
IC-FB-S	Feedback integrated control with handling of the switch of control period; T_{RM} = 30 s and T_{VSL} = 60 s.	7,301	−48.4
IC-FB	Feedback integrated control without handling of the switch of control period; T_{RM} = 30 s and T_{VSL} = 60 s.	7,405	−47.7
IC-FB-S'	Feedback integrated control with handling of the switch of control period; T_{RM} = 20 s and T_{VSL} = 60 s.	7,306	−48.4
IC-FB'	Feedback integrated control without handling of the switch of control period; T_{RM} = 20 s and T_{VSL} = 60 s.	7,385	−47.9

congestion at the bottleneck area just after the beginning of the simulation. The density is seen to remain overcritical ($\rho_{\mathrm{cr,L107}}$ = 32 veh/km/lane) during most of the simulation. The congestion propagates upstream (not shown), blocking several on-/off-ramps in the South and West portions of the ring-road, including the important junction with A4. This causes a reduction in throughput at the off-ramps and the formation of queues at the on-ramps, see, e.g., (Carlson et al., 2010a, 2013c). The flow at bottleneck of around 5,400 veh/h (Figure 6(a)) is below the nominal capacity ($q_{\mathrm{cap,L107}} \approx 5900$ veh/h) because of a capacity drop of around 8%. Despite of the formed congestion, the queue at OA1 does not exceed 50 veh. The TTS for this scenario is 14,163 veh·h. The described scenario is very similar to the real conditions on the motorway (Kotsialos et al., 2002).

4.3. Ramp Metering

For the application of RM, two cases are considered in order to highlight the effect of limited on-ramp storage space. In the first case, there is no queue constraint for the metered on-ramp (RM-FB), i.e., the on-ramp's storage capacity is unlimited. In the second case, the on-ramp storage space is limited and the metered on-ramp queue should not exceed $\hat{w}$ = 200 veh (RM/Q-FB). The PI-ALINEA gains are $\bar{K}_{\mathrm{P}}$ = 300 km·lane/h and $\bar{K}_{\mathrm{I}}$ = 120 km·lane/h, and the set-point is $\hat{\rho}_{\mathrm{out}}$ = 32 veh/km/lane.

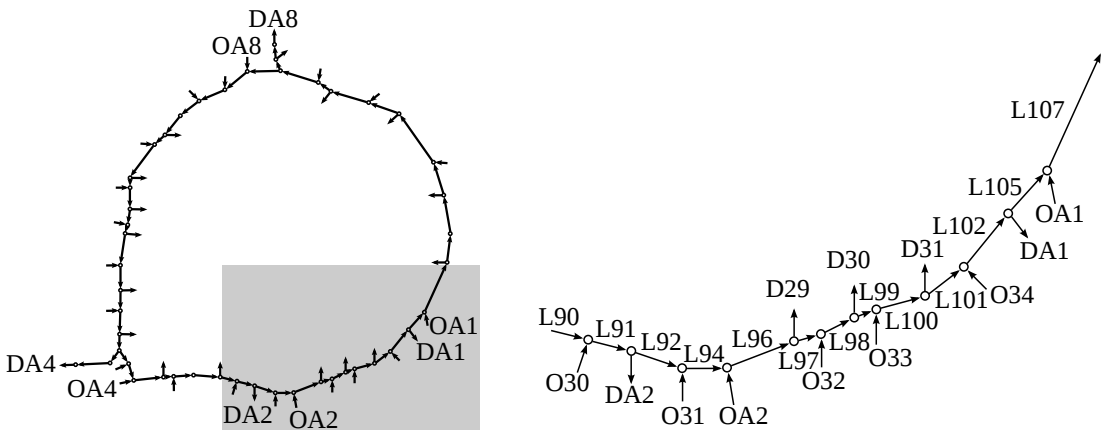

Figure 5: Amsterdam ring-road (A10).

4.3.1. Unlimited on-ramp storage space

The resulting TTS for RM-FB is 7,339 veh·h, which is a 48.2% improvement compared to the no-control case, and very close to the corresponding optimal control scenario (RM-AMOC). The density and flow at the bottleneck area (L107) and on-ramp queue at the on-ramp OA1 are shown in Figure 6(b) by the dark gray lines.

The density at the bottleneck area is maintained around the critical density (light gray line in the density plot), except when the demand is low, between t = 0.5 h and t = 1.5 h. As a consequence, the flow in the bottleneck area remains near capacity, which leads to a reduction in the TTS. To obtain this result, a queue is created at the on-ramp OA1 and, since there is no limitation in the queue length, it reaches almost 600 veh at around t = 2.7 h.

4.3.2. Limited on-ramp storage space

In the case of RM/Q-FB, the resulting TTS is 12,667 veh·h, which is a 10.6% improvement compared to the no-control case, but slightly worse than the corresponding optimal control scenario (RM/Q-AMOC). The performance is significantly worse than the case with unlimited on-ramp storage space at the on-ramp because RM is overridden by queue management. The density and flow at the bottleneck area (L107) and the ramp queue at the on-ramp OA1 are shown in Figure 6(b) by the black line. The light gray curve appearing in the queue plot corresponds to $\hat{w}$.

The situation is identical to the previous scenario until short before t = 0.2 h, when the on-ramp storage space is about to be exceeded, and queue management is activated so as to maintain the queue within the stipulated limits. As a consequence, the critical density at the bottleneck cannot be sustained anymore, in contrast to the case with unlimited storage space. Hence, congestion is formed thereafter, leading to a corresponding drop in the exit flow. The queue at the on-ramp is maintained around 200 veh, exceeding this value twice due to the formed congestion on the mainstream.

4.4. Mainstream Traffic Flow Control

MTFC-VSL using feedback control (MTFC-FB) is applied as described in Section 3.2. The VSL rate b delivered by the control law (3) is applied at links L101–L102 which correspond to the application area. Link L105 corresponds to the acceleration area. Due to safety reasons, additional VSLs are displayed upstream of the application area to

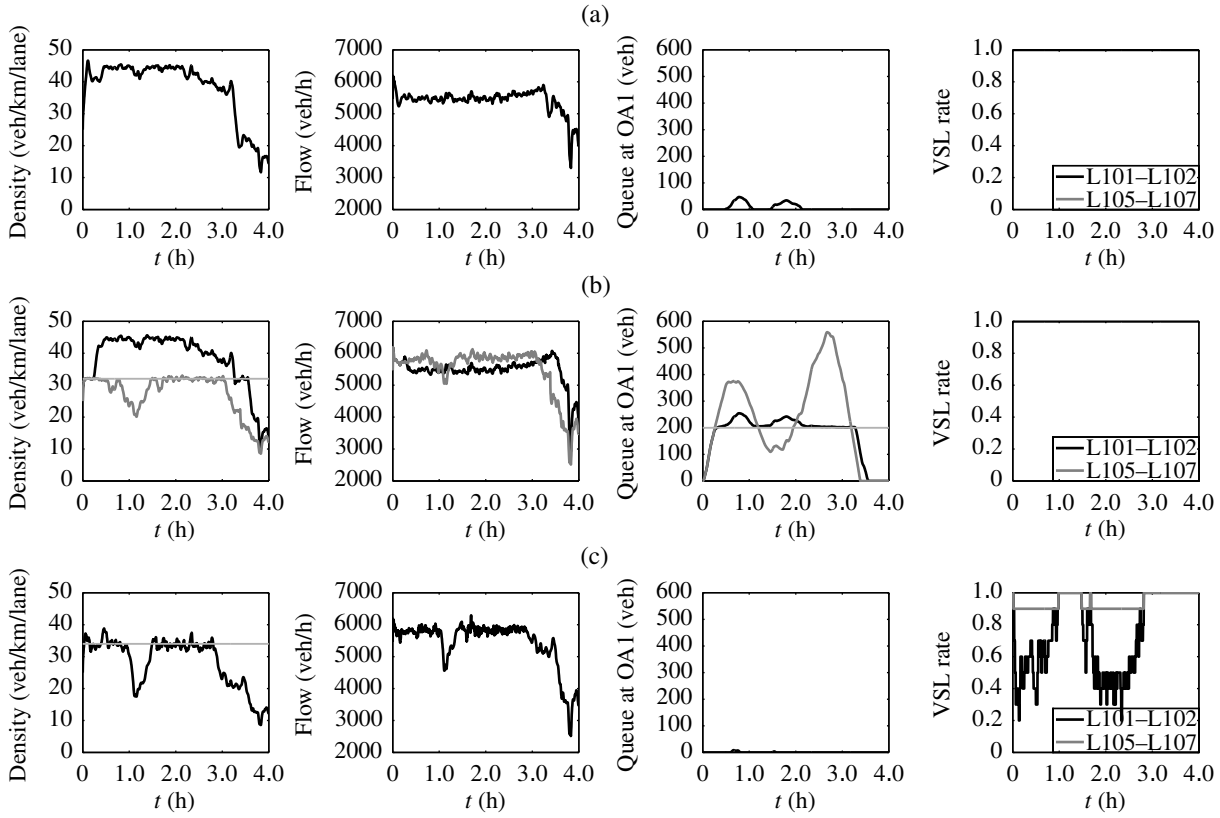

Figure 6: Density and flow at the bottleneck (L107), queue at the on-ramp OA1, and VSL rates at the application, acceleration and bottleneck areas (L101–L102 and L105–L107): (a) no-control; (b) feedback RM with (dark gray line) and without (black line) queue constraints; and (c) feedback MTFC-VSL.

avoid that vehicles reaching the controlled congestion encounter abrupt speed variations. Moreover, the VSL rates are discretized and their space-time variation is limited. The VSL rate at the acceleration and bottleneck areas is fixed at 0.9 (Carlson et al., 2011a). The measurement of density is obtained from L107, while the flow measurement is obtained from L105. The critical density at the bottleneck area serves as a reference for the primary controller and is $\hat{\rho}_{\text{out}}$ = 34 veh/km/lane, slightly higher than in the RM case (Section 4.3) because $b_{\text{L105–L107}}$ = 0.9. The controller gains are K_{I} = 0.0015 h·lane/veh for the secondary controller, and K'_{P} = 38 km/h and K'_{I} = 9 km/h for the primary controller. The resulting TTS is 9,513 veh·h, which is a 32.8% improvement compared to the no-control case and smaller than the corresponding optimal control scenario (MTFC-AMOC). This difference in performance between MTFC-FB and MTFC-AMOC is due to the blocking of off-ramps upstream of the bottleneck that is better managed by MTFC-AMOC, as discussed by Carlson et al. (2013c). The related density and flow at the bottleneck area (L107), the ramp queue at on-ramp OA1, and the VSL rates in L101–L102 and L105–L107 are shown in Figure 6(c).

In this scenario, the congestion at the bottleneck, and consequently the capacity drop, are completely avoided (Figure 6(c)) since the density remains around the critical value (reference), marked by the light gray line at the density plot. Controlled congestion (not shown) is formed upstream of the bottleneck location by the two control actions (VSL rate plot) and, being less intense than the no-controlled case, have a less negative effect on the

throughput at off-ramps and on the formation of queues at on-ramps. Note that in the RM-FB case the congestion on the mainstream is completely avoided and there are no off-ramp blockings, which justifies the better performance compared to MTFC-FB.

4.5. Integrated Control

When IC-FB-S is used, the resulting TTS is 7,301 veh·h, which corresponds to an improvement of 48.4% when compared to the no-control case, and is only 1% smaller than the corresponding optimal control case (IC-AMOC). The density and flow at the bottleneck area (L107), ramp queue at OA1, and the VSL rates in L101–L102 and L105–L107 are shown in Figure 7(a). The control gains and set-points are the same used in Sections 4.3 and 4.4, according to Section 3.3.

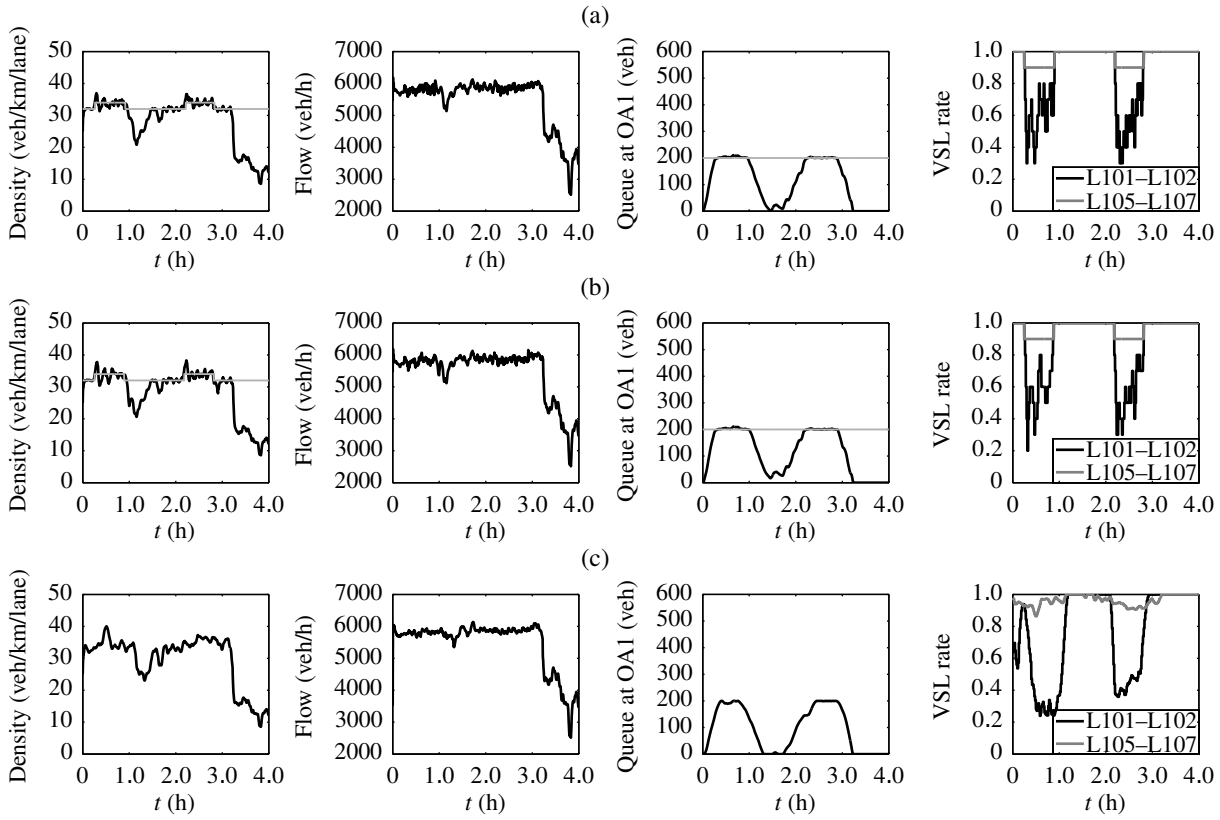

Figure 7: Density and flow at the bottleneck (L107), queue at the on-ramp OA1, and VSL rates at the application, acceleration and bottleneck areas (L101–L102 and L105–L107) with T_{VSL} = 60 s and T_{RM} = 30 s: (a) feedback integrated control with handling of the switching of the control period; (b) feedback integrated control without handling the switching of the control period; and (c) optimal integrated control.

IC-FB-S is capable of maintaining the density at the bottleneck area around the critical value (light gray line in the density plot) despite the restriction of 200 veh at the on-ramp queue. At around t = 0.2 h, the queue at OA1 reaches the value of 200 veh, and at about the same time the queue management overrides RM and integrated control continues operation as MTFC-VSL. Indeed, VSL is activated, and the reference is changed from 32 to 34 veh/km/lane to adjust to the VSL rate of 0.9 at the acceleration and bottleneck areas. When MTFC-VSL is no longer needed, at around t = 1.0 h, the critical density goes back to 32 veh/km/lane and the on-ramp queue starts

dissolving as RM becomes less restrictive. A similar behaviour is observed from $t = 2.0$ h. Since part of the traffic is held back at the on-ramp, the control effort required from MTFC-VSL in the integrated case is much smaller than in the stand-alone MTFC-VSL case (Figure 6(c)).

To illustrate the importance of the handling of the switch of control periods presented in Section 3.3.2, Figure 7(b) depicts the results in case the transition was ignored (IC-FB). Despite the small difference in TTS between the two scenarios (Table 1), the response in the IC-FB-S case is better damped. Note the smaller variations around the set-point after the switch at $t = 0.2$ h and the smaller overshoots at the switches at $t = 2.2$ h and $t = 2.8$ h.

The integrated optimal control (IC-AMOC) results depicted in Figure 7(c) show a similar trend as the integrated feedback case. Note that no splitting policy is imposed to AMOC, which optimizes freely the best combination of RM and VSL. Two aspects are noteworthy: (i) lower VSL values applied at L105–L107 are followed by increased densities at the bottleneck area and (ii) VSL control actions are stronger and more durable (starting earlier and releasing later) with AMOC and on-ramp queues at OA1 are shorter in time. The latter indicates that the pursued split policy for the feedback case is suboptimal.

Finally, the feedback results in Figure 7 are repeated in Figure 8, both with (IC-FB-S') and without (IC-FB') handling of the switching of the control period, but with $T_{\mathrm{VSL}} = 60$ s and $T_{\mathrm{RM}} = 20$ s (which also applies to queue management), i.e., $T_{\mathrm{VSL}} = 3T_{\mathrm{RM}}$. The integral gain corresponding to ramp metering operation (PI-ALINEA) was reduced accordingly to $\bar{K}_{\mathrm{I}} = 80$ km·lane/h. The respective TTS are shown in Table 1. Compared to the use of $T_{\mathrm{RM}} = 30$ s the differences are minor. The IC-FB-S' seems slightly less damped, possibly due to the approximated calculation of $\hat{q}_{\mathrm{t}}^{\mathrm{avg}}$.

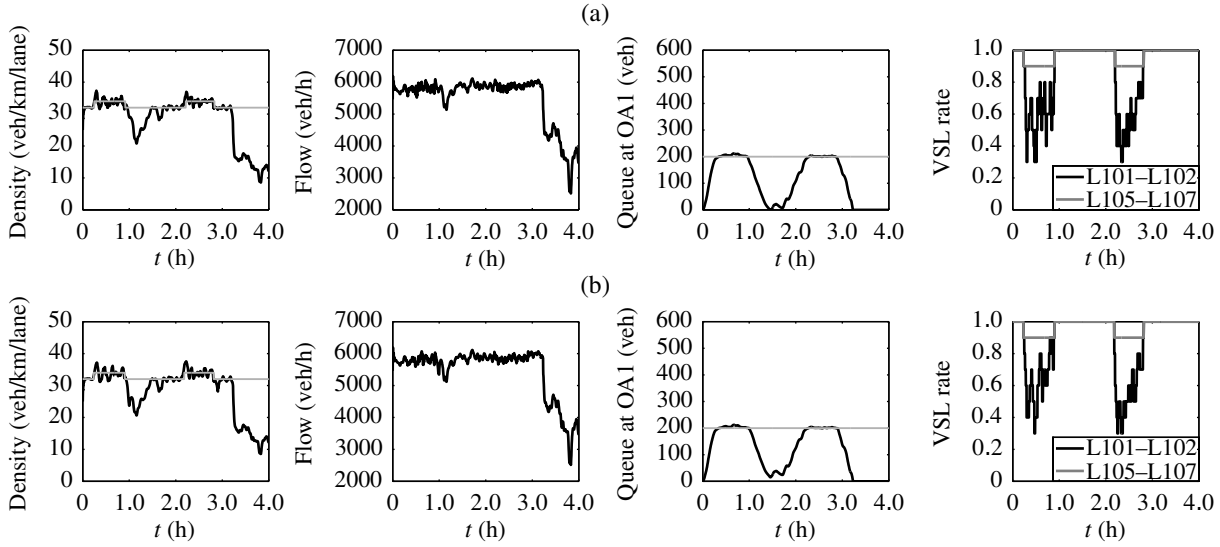

Figure 8: Density and flow at the bottleneck (L107), queue at the on-ramp OA1, and VSL rates at the application, acceleration and bottleneck areas (L101–L102 and L105–L107) with $T_{\mathrm{VSL}} = 60$ s and $T_{\mathrm{RM}} = 20$ s: (a) feedback integrated control with handling of the switching of the control period; and (b) feedback integrated control without handling the switching of the control period.

5. CONCLUSIONS

The integration of Mainstream Traffic Flow Control (MTFC) via Variable Speed Limits (VSL) and Ramp Metering (RM) for the efficient control of motorway traffic was presented based on techniques of feedback control. An existing cascade feedback MTFC-VSL controller was extended by use of a split-range-like scheme so as to allow integration with RM. The split control was designed in such a way that MTFC-VSL enters in operation only when the on-ramp queue is about to be exhausted or the RM lower bound has been reached. The proposed strategy considers the possibility of different control periods for MTFC-VSL and RM. The integrated feedback control strategy remains simple and yet efficient as evidenced by its evaluation using the METANET macroscopic traffic simulator and its comparison with non-integrated control and with an optimal control approach for the simulation model of a real motorway ring-road.

Ongoing research is investigating the integration of RM and MTFC at the network level (coordination), as well as the application of different splitting policies. A field test of the proposed strategy will be attempted in the near future.

Acknowledgements

At an early stage of this work the first author was supported by The Capes Foundation, Ministry of Education of Brazil, under Grant n. 23038.007817/2011-48. For the research leading to these results, the second and third authors have received funding from the European Research Council under the European Union's Seventh Framework Programme (FP/2007-2013)/ERC Grant Agreement n. 321132, project TRAMAN21.

References

Albertos, P., Vallés, M., Valera, A., 2003. Controller transfer under sampling rate dynamic changes, in: Proceedings of the European Control Conference, Cambridge, UK.

Carlson, R.C., Manolis, D., Papamichail, I., Papageorgiou, M., 2012a. Integrated ramp metering and mainstream traffic flow control on freeways using variable speed limits. Procedia - Social and Behavioral Sciences 48, 1578–1588. doi:10.1016/j.sbspro.2012.06.1133.

Carlson, R.C., Manolis, D., Papamichail, I., Papageorgiou, M., 2012b. Integrated ramp metering and mainstream traffic flow control on freeways using variable speed limits, in: Proceedings of The 13th IFAC Symposium on Control in Transportation Systems, Sofia, Bulgaria. pp. 110–115. doi:10.3182/20120912-3-BG-2031.00021.

Carlson, R.C., Papamichail, I., Papageorgiou, M., 2011a. Local feedback-based mainstream traffic flow control on motorways using variable speed limits. IEEE Transactions on Intelligent Transportation Systems 12, 1261–1276. doi:10.1109/TITS.2011.2156792.

Carlson, R.C., Papamichail, I., Papageorgiou, M., 2013a. Comparison of local feedback controllers for the mainstream traffic flow on freeways using variable speed limits. Journal of Intelligent Transportation Systems 17, 268–281. doi:10.1080/15472450.2012.721330.

Carlson, R.C., Papamichail, I., Papageorgiou, M., 2013b. Controle integrado de acesso e do fluxo principal em rodovias, in: Panorama Nacional de Transportes 2013, ANPET, Belém.

Carlson, R.C., Papamichail, I., Papageorgiou, M., 2013c. Mainstream traffic flow control on freeways using variable speed limits. Transportes 21, 56–65. doi:10.4237/transportes.v21i3.694.

Carlson, R.C., Papamichail, I., Papageorgiou, M., Messmer, A., 2010a. Optimal mainstream traffic flow control of large-scale motorway networks. Transportation Research Part C: Emerging Technologies 18, 193–212. doi:10.1016/j.trc.2009.05.014.

Carlson, R.C., Papamichail, I., Papageorgiou, M., Messmer, A., 2010b. Optimal motorway traffic flow control involving variable speed limits and ramp metering. Transportation Science 44, 238–253. doi:10.1287/trsc.1090.0314.

Carlson, R.C., Ragias, A., Papamichail, I., Papageorgiou, M., 2011b. Mainstream traffic flow control of merging motorways using variable speed limits, in: Proceedings of The 19th Mediterranean Conference on Control and Automation, IEEE, Corfu, Greece. pp. 674–681. doi:10.1109/MED.2011.5983115.

Chang, H., Wang, Y., Zhang, J., Ioannou, P., 2007. An integrated roadway controller and its evaluation by microscopic simulator VISSIM, in: Proceedings of The European Control Conference, Kos, Greece. pp. 2436–2441.

Fadali, M.S., Visioli, A., 2013. Digital Control Engineering: Analysis and Design. 2 ed., Academic Press, Boston.

Hegyi, A., De Schutter, B., Hellendoorn, H., 2005a. Model predictive control for optimal coordination of ramp metering and variable speed limits. Transportation Research Part C: Emerging Technologies 13, 185–209. doi:10.1016/j.trc.2004.08.001.

Hegyi, A., De Schutter, B., Hellendoorn, J., 2005b. Optimal coordination of variable speed limits to suppress shock waves. IEEE Transactions on Intelligent Transportation Systems 6, 102–112. doi:10.1109/TITS.2004.842408.

Hegyi, A., Hoogendoorn, S., Schreuder, M., Stoelhorst, H., Viti, F., 2008. SPECIALIST: a dynamic speed limit control algorithm based on shock wave theory, in: 2008 11th International IEEE Conference on Intelligent Transportation Systems, Beijing, China. pp. 827–832. doi:10.1109/ITSC.2008.4732611.

Hegyi, A., Hoogendoorn, S.P., 2010. Dynamic speed limit control to resolve shock waves on freeways - field test results of the SPECIALIST algorithm, in: 13th International IEEE Conference on Intelligent Transportation Systems, Funchal, Madeira Island, Portugal. pp. 519–524. doi:10.1109/ITSC.2010.5624974.

Karimi, A., Hegyi, A., De Schutter, B., Hellendoorn, J., Middelham, F., 2004. Integrated model predictive control of dynamic route guidance information systems and ramp metering, in: The 7th International IEEE Conference on Intelligent Transportation Systems, 2004., IEEE, Washington, D.C., USA. pp. 491–496. doi:10.1109/ITSC.2004.1398949.

Kotsialos, A., Papageorgiou, M., Mangeas, M., Haj-Salem, H., 2002. Coordinated and integrated control of motorway networks via non-linear optimal control. Transportation Research Part C: Emerging Technologies 10, 65–84. doi:10.1016/S0968-090X(01)00005-5.

Lu, X.Y., Varaiya, P., Horowitz, R., Su, D., Shladover, S.E., 2010. A new approach for combined freeway variable speed limits and coordinated ramp metering, in: 13th International IEEE Conference on Intelligent Transportation Systems, Funchal, Madeira Island, Portugal. pp. 491–498. doi:10.1109/ITSC.2010.5625107.

Messmer, A., Papageorgiou, M., 1990. METANET: a macroscopic simulation program for motorway networks. Traffic Engineering and Control 31, 466–470.

Müller, E.R., Carlson, R.C., Kraus, W., Papageorgiou, M., 2013. Microscopic simulation analysis of mainstream traffic flow control with variable speed limits, in: 16th International IEEE Conference on Intelligent Transportation Systems, IEEE. pp. 998–1003. doi:10.1109/ITSC.2013.6728362.

Papageorgiou, M., Diakaki, C., Dinopoulou, V., Kotsialos, A., Wang, Y., 2003. Review of road traffic control strategies. Proceedings of the IEEE 91, 2043–2067. doi:10.1109/JPROC.2003.819610.

Papageorgiou, M., Haj-Salem, H., Blosseville, J.M., 1991. ALINEA: a local feedback control law for on-ramp metering. Transportation Research Record 1320, 58–64.

Papageorgiou, M., Kosmatopoulos, E., Papamichail, I., 2008. Effects of variable speed limits on motorway traffic flow. Transportation Research Record: Journal of the Transportation Research Board 2047, 37–48. doi:10.3141/2047-05.

Papageorgiou, M., Kotsialos, A., 2002. Freeway ramp metering: an overview. IEEE Transactions on Intelligent Transportation Systems 3, 271–281. doi:10.1109/TITS.2002.806803.

Papageorgiou, M., Papamichail, I., 2008. Overview of traffic signal operation policies for ramp metering. Transportation Research Record: Journal of the Transportation Research Board 2047, 28–36. doi:10.3141/2047-04.

Papamichail, I., Kotsialos, A., Margonis, I., Papageorgiou, M., 2010. Coordinated ramp metering for freeway networks - a model-predictive hierarchical control approach. Transportation Research Part C: Emerging Technologies 18, 311–331. doi:10.1016/j.trc.2008.11.002.

Papamichail, I., Papageorgiou, M., 2011. Balancing of queues or waiting times on metered dual-branch on-ramps. IEEE Transactions on Intelligent Transportation Systems 12, 438–452. doi:10.1109/TITS.2010.2093130.

Pohjola, M., 2009. Adaptive control speed based on network quality of service, in: 17th Mediterranean Conference on Control and Automation, IEEE. pp. 784–789. doi:10.1109/MED.2009.5164639.

Schelling, I., Hegyi, A., Hoogendoorn, S.P., 2011. SPECIALIST-RM: integrated variable speed limit control and ramp metering based on shock wave theory, in: Proceedings of the 14th International IEEE Conference on Intelligent Transportation Systems, IEEE. pp. 2154–2159. doi:10.1109/ITSC.2011.6083116.

Smaragdis, E., Papageorgiou, M., 2003. Series of new local ramp metering strategies. Transportation Research Record 1856, 74–86. doi:10.3141/1856-08.

Stephanopoulos, G., 1984. Chemical Process Control: an Introduction to Theory and Practice. Prentice-Hall, Englewood Cliffs N.J.

Sun, X., Horowitz, R., 2005a. A localized switching ramp-metering control with queue length estimation and microscopic simulation results, in: Proceedings of the 16th IFAC World Congress, 2005, Prague, Czech Republic. doi:10.1109/ACC.2005.1470287.

Sun, X., Horowitz, R., 2005b. A localized switching ramp-metering controller with a queue length regulator for congested freeways, in: Proceedings of the 2005 American Control Conference, Portland, OR, USA. pp. 2141–2146. doi:10.1109/ACC.2005.1470287.

Vigos, G., Papageorgiou, M., Wang, Y., 2008. Real-time estimation of vehicle-count within signalized links. Transportation Research Part C: Emerging Technologies 16, 18–35. doi:10.1016/j.trc.2007.06.002.

Wang, Y., Kosmatopoulos, E.B., Papageorgiou, M., Papamichail, I., 2014. Local ramp metering in the presence of a distant downstream bottleneck: Theoretical analysis and simulation study. IEEE Transactions on Intelligent Transportation Systems , 1–16URL: http://dx.doi.org/10.1109/TITS.2014.2307884, doi:10.1109/TITS.2014.2307884.

Zegeye, S.K., De Schutter, B., Hellendoorn, J., Breunesse, E.A., Hegyi, A., 2012. A predictive traffic controller for sustainable mobility using parameterized control policies. IEEE Transactions on Intelligent Transportation Systems 13, 1420–1429. doi:10.1109/TITS.2012.2197202.

Zhang, J., Chang, H., Ioannou, P.A., 2006. A simple roadway control system for freeway traffic, in: 2006 American Control Conference, Minneapolis, MN, USA. pp. 4900–4905. doi:10.1109/ACC.2006.1657497.